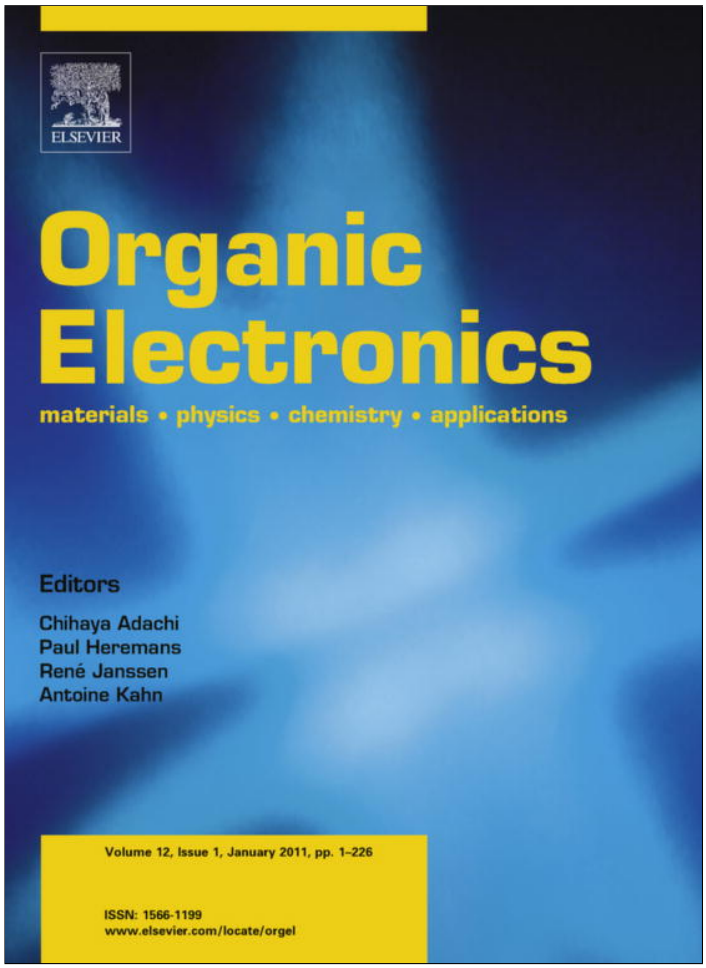

(This is a sample cover image for this issue. The actual cover is not yet available at this time.)

Organic Electronics 12 (2011) 851–856

Contents lists available at ScienceDirect

Organic Electronics

journal homepage: www.elsevier.com/locate/orgel

Doping and photo-induced current in discotic liquid crystals thin films: Long-time and temperature effects

Annalisa Calò [a], Pablo Stoliar [a], Massimiliano Cavallini [a,*], Yves H. Geerts [b], Fabio Biscarini [a,*]

[a] National Research Council of Italy (CNR), Institute for the Study of Nanostructured Materials (ISMN), Via P. Gobetti 101, I-40129 Bologna, Italy
[b] Laboratoire de Chimie des Polymères CP 206/1, Faculté des Sciences, Université Libre de Bruxelles (ULB), Boulevard du Triomphe, 1050 Bruxelles, Belgium

ARTICLE INFO

Article history:
Received 3 January 2011
Received in revised form 10 February 2011
Accepted 10 February 2011
Available online 3 March 2011

Keywords:
Discotic liquid crystals
Photocurrent
Time and temperature stability

ABSTRACT

Here we address the problem of time and temperature instability of the electrical current related to parasitic doping effects in discotic liquid crystals (DLCs). We investigated the electrical transport in thin films of a phthalocyanine-based DLC in-dark and upon laser irradiation during long thermal cycles. Measuring the electrical transport between two electrodes we observed that in-dark the current is mostly due to doping levels while, upon laser irradiation, the photocurrent reflects the diffusion length of the photogenerated charge carriers and it is limited by the coherence length of a column. We prove here that the two contributions are completely independent. Our result experimentally supports the theoretical studies performed at the molecular level on discotic liquid crystals.

1. Introduction

Discotic liquid crystals (DLCs) [1] are a class of liquid crystals proposed for many applications in organic electronics [2–5], including organic field effect transistors (OFETs) [6,7], in photovoltaics [8–10], as sensors [11,12] and in information storage [12]. DLCs are formed by a rigid aromatic core and highly flexible peripheral chains, which provide solubility and drive self-organizing properties of these materials in columns forming different mesophases [13,14].

The relevant properties arise from their self-assembling behavior governed by a combination of the strong π–π overlap between individual molecules [15] and the interaction of peripheral functional groups, which allow the formation of the columnar mesophases [13–16].

Many theoretical studies have been performed in order to extract the molecular parameters that have direct influence on the electrical transport [5,17–19]. Although a good coupling interaction is predicted between two discotic molecules [20,21] and hence an optimum intermolecular charge transfer is expected, actual devices fabricated with DLCs semiconductors exhibit relatively poor performances, attributed to static and dynamic disorder [22] and to the one-dimensional character of charge transport that renders DLCs a very sensitive system to defects and impurities [16].

In particular a severe limit to their application in electronic devices is determined by the time and temperature instability of the electrical response related to parasitic doping effects. Here we address this problem by studying the electrical transport in thin films of a phthalocyanine mesogen [20] in-dark conditions and upon laser irradiation during long thermal cycles performed at a controlled rate.

The characterization of these materials in devices has been performed by several methods, including Pulse-Radiolysis Time Resolved Microwave Conductivity, Time-of-Flight transient photoconductivity, space charged limited current measurements [4,23]. Electrical characterization of transistors [24,25] is reported as well as the integration of DLCs in photovoltaic junctions [26] and in-between interdigitated electrodes [27].

All these experiments have been performed by measuring the photo- and dark-current separately using different

* Corresponding authors. Tel.: +39 0516398516 (M. Cavallini).
E-mail addresses: m.cavallini@bo.ismn.cnr.it (M. Cavallini), f.biscarini@bo.ismn.cnr.it (F. Biscarini).

1566-1199/$ - see front matter © 2011 Elsevier B.V. All rights reserved.
doi:10.1016/j.orgel.2011.02.007

methods and comparing in some cases the two different contributions [3]. No direct correlation between the contributions in-dark and in-light to the electrical properties has been reported as measured on the same device.

It is known that the electrical conduction in liquid crystals and in particular in phthalocyanine-based materials is greatly affected by contaminants and environmental conditions [11,28–32]. Although a controlled doping produces a strengthening of the sensing capability, it becomes a major limitation in organic electronics applications. The amount of contaminants is less controllable when the films are deposited or cast starting from solutions, where the solvent itself or the process can provide dopants, determining unstable electrical response.

2. Experiments, results and discussion

In our work we simultaneously measured the photocurrent and the current in-dark vs. time and temperature. These measurements allow us to assess the instability of the electrical measurements and the influence of contaminants on the electrical device response.

Here we used a metal-free mesogenic phthalocyanine 2(3),9(10),16(17),23(24)-tetra(2-decyltetradecyloxy)-phthalocyanine (H_2Pc) (Fig. 1), containing very low level of ionic impurities (see Supporting information of Ref. [20]). H_2Pc is a prototype DLC compound exhibiting a columnar rectangular (Col_r) ↔ columnar hexagonal (Col_h) phase transition at T_{rh} = 333 K [33].

When a H_2Pc thin film is deposited onto a surface, in general the planar alignment of columns is spontaneously achieved regardless of the nature of the surface [33]. We performed the experiment on a thin film of H_2Pc deposited in-between two interdigitated electrodes on a test pattern with a bottom-contact layout (Fig. 2) using a sourcemeter–femtoammeter to bias the device and measure the DC current flow. Details of set-up is described in Ref. [34]. We biased the device with a voltage V = 5 V and acquired current measurements repeating thermal cycles between 303 K and 363 K at a controlled rate of 1.0 K/min. We chose this range because it is the most common condition of working temperatures without relevant effects on reorganization or on electrically induced dewetting [27];

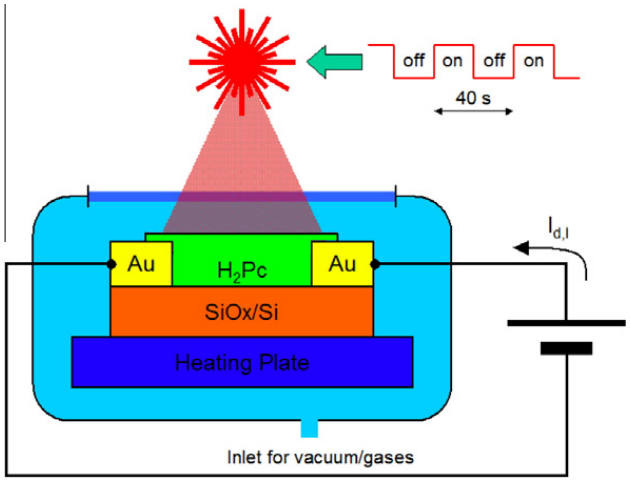

Fig. 2. Experimental setup, including the heating stage and the laser, which illuminates the sample with intermittent light during the thermal cycles.

furthermore within this range the Col_r–Col_h phase transition is expected [20]. All the measurements were performed in vacuum (P = 0.01 mbar) by illuminating the film during the thermal cycles with an intermittent light (frequency = 1/40 s) whose 680 nm wavelength is near to the maximum absorption of H_2Pc [20]. The experiment output is a set of alternating dark and light (indicated as I_d and I_l, respectively) DC current measurements.

Fig. 3a shows the I_d measurement. The triangular shape of the projection in the (t, T) plane represents the temperature sweep performed by the heating stage, assuming t_0 = 0 at 303 K as starting point and using a heating/cooling rate of 1 K/min (thus arriving to the temperature of 363 K after 1 h); the temperature is then returned to 303 K and the cycle is repeated 10.5 times. In Fig. 3b the corresponding I_l values are shown. With an interpolation routine (see methods) we generated the I_d (t, T) and the I_l (t, T) surfaces presented in Fig. 3a and b. By subtracting I_d from the corresponding I_l values we extracted the photocurrent contribution (I_p), which is due to excited H_2Pc states generated by light absorption (Fig. 3c) [35]. The noise level in the I_l and I_d measurements was less than 6pA rms, making the calculated values of I_p at least 11 times bigger than its

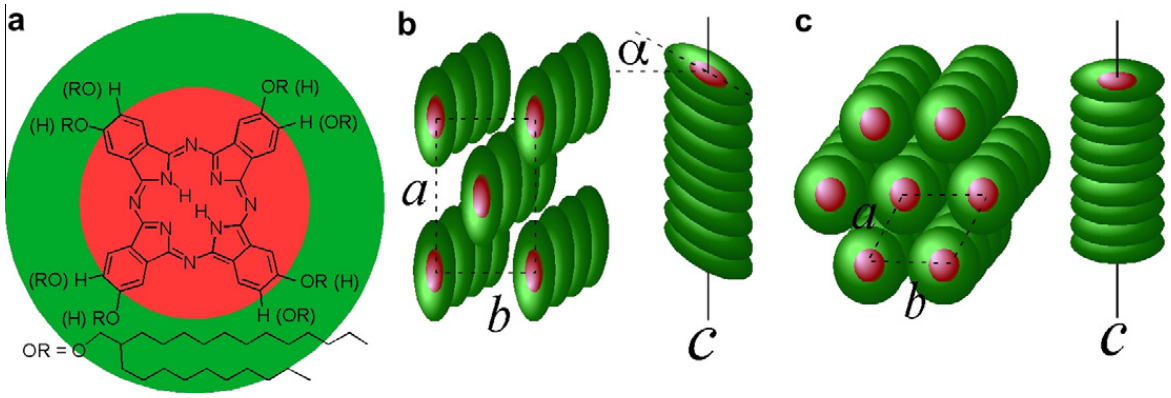

Fig. 1. (a) Chemical structure of 2(3),9(10),16(17),23(24)-tetra(2-decyltetradecyloxy)-phthalocyanine (H_2Pc). (b) Columnar rectangular and (c) columnar hexagonal organization. a, b, c are the cell parameters [17,30] and α is the tilt angle with respect to the column axis.

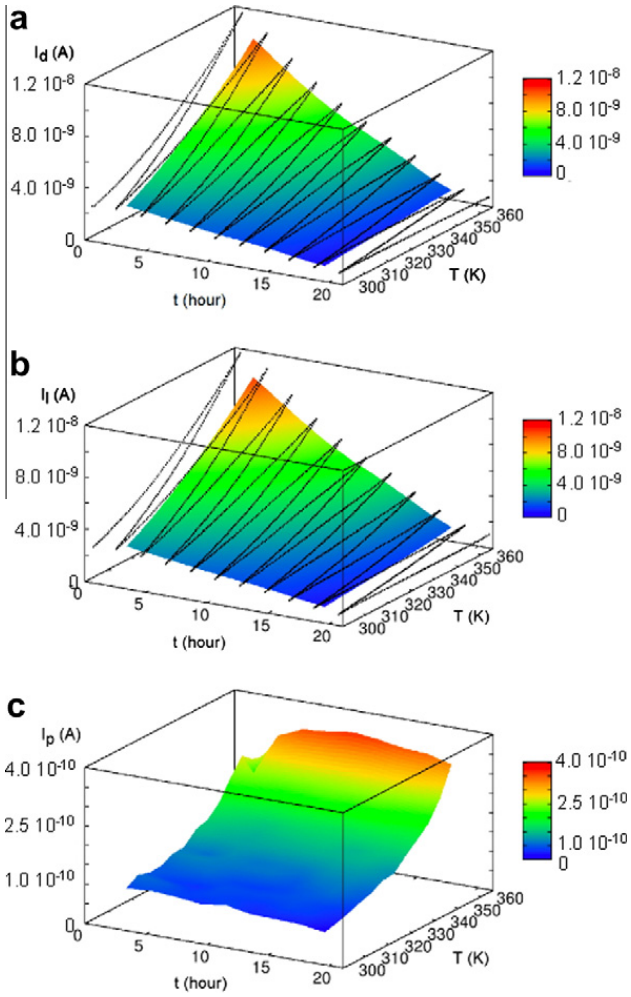

Fig. 3. Surfaces of current in-dark (I_d) (a), during laser irradiation (I_l) (b) and photocurrent contribution (I_p) (c) vs. time and temperature measured in vacuum.

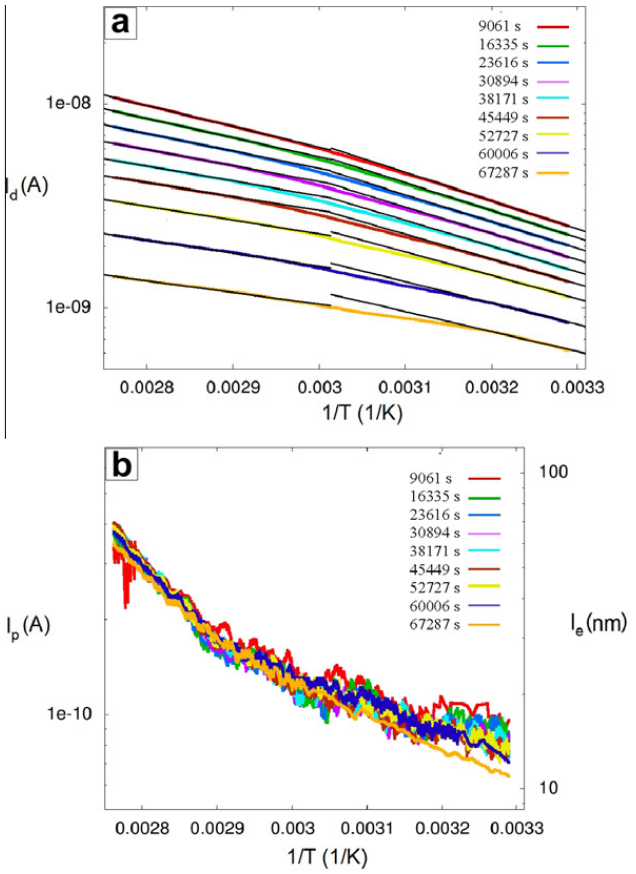

Fig. 4. Dependence of current in-dark (I_d) (a), photocurrent contribution (I_p) (b, left axis) and photogenerated charge carriers diffusion length (l_e) (b, right axis) from the absolute temperature for fixed times (A = 9061 s, B = 16,335 s, C = 23,616 s, D = 30,894 s, E = 38,171 s, F = 45,449 s, G = 52,727 s, H = 60,006 s, I = 67,287 s).

indetermination $\sigma_{Ip} = \sqrt{2} \cdot \sigma_{Id}$ (see details of error analysis in Section 4.5).

We find that I_p is almost independent on time, in contrast with I_d (t, T) and I_l (t, T).

Fig. 4a shows sections of the surface I_d (t, T) performed at intervals of 2 h in an Arrhenius plot.

We identified two different activated regimes corresponding to each liquid crystalline phase:

$$I_d = \begin{cases} A_r \cdot \exp(-\frac{E_r}{k_B T}) & T < T_{rh}; \\ A_h \cdot \exp(-\frac{E_h}{k_B T}) & T > T_{rh}. \end{cases} \quad (1)$$

The prefactor A_r and the activation energy E_r belong to the Col_r phase, while A_h and E_h to the Col_h phase. T_{rh} is the temperature of the Col_r–Col_h phase transition. We identified the two regimes and we extracted the prefactors and the activation energies without fixing a priori T_{rh}. Then we calculated the temperature where the two lines in the Arrhenius plot corresponding to the two regimes of Eq. (1) intersect each other. This temperature (328.40 ± 5.07) K is in good agreement with the DSC results (331.45 K) [36].

Both A_r and A_h decrease in time with a decay constant of respectively 6420 (±590) s and 5451 (±146) s. From the fit according to Eq. (1) we extracted $E_r = (0.245 \pm 0.024)$ eV and $E_h = (0.153 \pm 0.030)$ eV. Assuming the Drude model, the in-dark current is given by:

$$I_d = q \cdot p(t,\ T) \cdot \mu_p \cdot V \cdot d \cdot W \cdot L^{-1} \quad (2)$$

where q is the elementary charge, $p(t, T)$ the number density of holes, μ_p their mobility, V is the electrical potential and d, W, L, the channel height, width and length, respectively.

By performing experiments in different atmospheric conditions (air, N_2, H_2O_2 vapours), thus in very different doping conditions, we obtained similar value of E_r and E_h.

Since in our range of T, μ_p is almost constant or weakly dependent on temperature [5] and time [20,21], the change of I_d with time and temperature can be ascribed to the change (decrease) of doping levels and possibly to the reorganization of ionic impurities inside the H_2Pc thin film [32].

The holes responsible for the electrical p-conduction are induced in the HOMO level by the presence an acceptor level introduced by doping [37]. This acceptor level is distant from the HOMO by E_r and E_h, depending on temperature. The change of activation energy at the Col_r–Col_h transition can be assigned to the stacking of H_2Pc molecules. In the Col_r mesophase, the normal to the disk-like molecules is

tilted by $\alpha = 15–18°$ vs. the column axis, whereas in Col_h mesophase is parallel [20]. The two supramolecular arrangements impose different overlaps between stacked molecules that finally impact on the energy of the HOMO level and consequently on its distance in energy with respect to the acceptor level.

The prefactors A_r and A_c are proportional to the doping level (number of acceptor states) in the film [38,39]. The fact that they decay in time can be interpreted as after the fabrication process relatively a high level of doping remains in the film. This is consistent with oxygen doping from air. By keeping the film in vacuum during the thermal cycles, the contaminants are progressively removed (evaporated).

By exciting the H_2Pc molecules in the film with the laser electron–holes pairs are generated [20,35] and their contribution to the current is independent from the doping level introduced during the film growth. The following equation for the photocurrent flowing between the electrodes in the case of intrinsic semiconductors applies [40]:

$$I_p = q \cdot \eta \cdot \frac{P_{opt}}{h\nu} \cdot \frac{(\mu_n + \mu_p) \cdot \tau \cdot V}{L^2} \tag{3}$$

where η is the quantum efficiency (i.e.; number of carriers generated per photon absorbed), P_{opt} the optical power, h the Planck constant, ν the frequency of the incident photons, τ the carriers lifetime, μ_{n-p}, respectively the electrons and holes mobility and L the channel length, viz. the distance between the electrodes. $q \cdot \eta \cdot P_{opt} \cdot (h \cdot \nu)^{-1}$ is the primary photocurrent.

Considering that the photogenerated charge carriers diffusion length l_e is the distance travelled by the carriers with a drift velocity $\langle v_n \rangle + \langle v_p \rangle = (\mu_n + \mu_p) \cdot V \cdot L^{-1}$ during their lifetime τ, the relationship between the diffusion length and the channel length is equal to the ratio between the measured photocurrent and the primary photocurrent:

$$\frac{\langle l_e \rangle}{L} = \frac{I_p}{q \cdot \eta \cdot \frac{P_{opt}}{h\nu}} \tag{4}$$

Fig. 4b shows the plot of I_p and l_e vs. temperature. l_e is obtained upon re-scaling the time-sections of the surface $I_p(t, T)$ by the constant factor $L \cdot q^{-1} \cdot \eta^{-1} \cdot P_{opt}^{-1} \cdot h\nu$, assuming a quantum efficiency $\eta = 0.5\%$, which is the value reported in Ref. [16] for phthalocyanines. The diffusion length increases with temperature, varying from 10 to 70 nm. This value, of the order of few hundreds molecular cores, is consistent with the reported excitons migration length [41] and intra column coherence length (150 nm) obtained by XRD [42] on DLCs.

We systematically observed two activated regimes in the I_p vs. temperature plot, but we did not find a significant correlation with the temperature of the Col_r–Col_h phase transition. Applying the same analysis as the one reported for I_d, we extracted a temperature of 344 ± 3 K for the example of Fig. 4b, and a mean value of 339 ± 10 K among different experiments performed in vacuum. Noticeably, in contrast with the measurements in-dark, we systematically observed that the average activation energy at low temperatures $E_{LT}^{p} = 0.125 \pm 0.047$ eV is smaller than the activation energy at high temperatures $E_{HT}^{p} = 0.509 \pm 0.067$ eV.

Furthermore, also in the case of the I_p curves, tiny fluctuations in the transport properties are present that seem to be correlated with the elapsed time. In Fig. 4b a small change in the local slope at the lowest temperatures is observed, suggesting slow reorganization dynamics affecting the photocurrent at these temperatures. From the linear fits in the range $0.0031–0.0033\ K^{-1}$ the slopes increase of about three times, from -737.4 K at 9061 s to -2387.1 K at 67,287 s. This behaviour is not systematic, either for the direction of the slope change or for the temperature range in which it occurs; it is still under investigation.

3. Conclusions

In conclusion we observed that the two measurements of DC current in-dark and photocurrent exhibit a very different behaviour with respect to the functional form and the stability over time and temperature.

The measurement in-dark is characterized by two activation energies that depend on the liquid crystalline phase, indicating a different relative position between the HOMO and the acceptor levels for each phase. The acceptor level can be introduced by doping during the fabrication process. Doping levels are mainly responsible for the conductivity of the film in-dark conditions, causing instabilities in the electrical measurements because during the experiment the contaminants are partially removed by evaporation or they reorganize [32]. This instability is particularly influent when the timescale for reorganization of dopants is comparable with the time scale of the temperature sweep. For this reason it is crucial to perform a procedure of interpolation, which leads to a time correction of the current vs. temperature curves in order to extract instantaneous $I_d(T)$ curves, as indicated here.

On the other hand, the functional form of the measurements at light reflects the photogenerated charge carriers diffusion length, which seems to be not much correlated with the film phase [20]. The amount of carriers in the photocurrent measurements is generated with the laser and is constant with temperature, in contrast to the measure in-dark, where the carriers are promoted by thermal excitation from acceptor states. The electric field separates the photo-generated carriers and the behaviour of I_p vs. temperature reflects the variation in the distance that carriers travel unperturbed until they find a structural defect or a trap. This distance can be indeed considered as the coherence (correlation) length of a column; we did not find any significant change of regime in the diffusion length of the photogenerated charge carriers that could be correlated with the phase transition. The observation that the current in-dark decreases in time (Fig. 3a), while the photocurrent contribution remains stable (Fig. 3c), suggests that the decay of I_d in time is not due to degradation of the material during the experiment. Here we used H_2Pc as representative material; however our approach is general and can be extended to other liquid crystals and more in general to other classes of organic materials such as molecular [43,44] or polymeric [45,46] semiconductors.

4. Experimental details

4.1. Substrate cleaning and film preparation

The test pattern is made up of a highly doped Si layer of 0.5 mm, with a 1 μm thick layer of thermal SiO*x*. The Au interdigitated electrodes are fabricated by photolithography and have a thickness of 150 nm. This test pattern was provided by Philips Research Laboratory, Eindhoven, The Netherlands. It features four devices with channel length equal to 10 μm and channel width equal to 10 mm.

We washed the test pattern with Heptane (HPLC grade) and we dry it with pure Nitrogen; then we washed it with Acetone (HPLC grade), drying with pure Nitrogen. We finally dip the test pattern in HF 4% for 20 s, washed it with electronic grade water and then dried it with pure Nitrogen. We put the substrate in an air plasma chamber (PELCO easiGlow 91000) for 10 min, setting $I = 30$ mA and $P = 0.4$ mbar.

After the cleaning procedure we deposited the H_2Pc film by spin coating from a 20 mg/mL solution in heptane (HPLC grade), setting the angular velocity to 2000 rpm. With these conditions we obtained a film 130 nm thick. We attached the film to the sample holder of the heating stage and made the electrical connections with silver paint. We baked the film at 313 K in vacuum ($P = 0.01$ mbar) for 30 min, then we heated it up to 456 K in order to induce the columnar organization, that we verified by optical microscopy using cross polarizers filters. We performed the same experiment described in the text on H_2Pc films in different ambient conditions, verifying the film stability during the experiment by using an optical microscope.

4.2. Determination of optical power transferred to the film (P_{opt}) and sample overheating by laser irradiation

To excite the sample we used a standard 680 nm laser diode with a nominal optical power of 1 mW coupled to a variable focus optic system. We determined the power deposited in the film P_{opt} using the formula:

$$P_{opt} = P_{laser} \cdot Ads \cdot L \cdot W \cdot s_{spot}^{-1} = 2.1 \cdot 10^{-5} W \quad (5)$$

where P_{laser} is the total power emitted by the laser in a spot of surface s_{spot}, $L{\cdot}W$ is the sensitive area of the device and Ads is the relation between the power transferred to the film and the power that arrives to the surface, i.e. excludes the power that is transferred to the substrate or reflected out of the sample. We measured the actual $P_{laser} = 0.4$ mW using a photodiode Thorlabs, Inc. model DET36A. We regulated the area of the spot to cover all the sensitive area of the device; then we measure $s_{spot} = 0.7 \times 10^{-6}$ m^2 from an image taken using the optical microscope. Also we took periodically images with the microscope to verify that the position of the laser remains unchanged during the experiment. To determine Ads we made a Monte Carlo simulation of the photons trajectory. It considers 10^7 photons arriving to a system which is made up of four layers: (1) air with an absorption coefficient $\alpha = 0$ and refractive index $n = 1$; (2) a 130 nm thick H_2Pc layer with $\alpha = 4.2 \cdot \times 10^4$ cm^{-1} and $n = 2.66$ [47]; (3) a 1 μm thick SiO*x* layer with $\alpha = 10$ cm^{-1} and $n = 1.46$; and (4) a 0.5 mm thick Si layer with $\alpha = 3 \times 10^3$ cm^{-1} and $n = 3.5$.

This simulation considers reflections at the interfaces and light attenuation in the different layers. The percentage of the laser power is distributed as follows: 37.1(6)% remains in the H_2Pc film, 0.0476(2)% in the SiO*x* layer, and 38.7(3)% in the Si layer. The remaining 24.1(5)% is reflected out of the sample.

Using these results we estimated that the increase of temperature between the bottom of the Si substrate and the H_2Pc top interface is less than 1 mK using a 1-D heat transmission model.

4.3. Experimental setup

The measurement system is based on a heating stage (Linkham TMHS600). We replaced one of the gas inlets of the heating stage with a feed through that allows the electrical connections from the sample to the sourcemeter. We used the stage input for vacuum/gases to control the atmosphere in the chamber. The stage is connected to a TP94 controller, a Keithley 6430 sourcemeter–femtammeter and a laser connected to a Keithley 3930A function generator. We substituted the optics of the laser diode with a 3.3 Macro Zoom lens (Edmund Optics) to regulate the focal distance between the laser and the sample, illuminating completely the active area of the device.

The TP94 controller is connected to the computer through a RS232 interface. The Keithley 6430 and the Keithley 3930A are connected to the computer through an IEEE-488 Bus. In this configuration we are able to set from the computer a temperature ramp, to set the voltage, to take at pre-set intervals an electrical measurement of current and to control the laser intensity on the sample, alternating dark–light cycles.

4.4. Generation of I_d, I_l and I_p surfaces

The measurement cycles give alternating I_d and I_l data at intervals of 0.3 K. Performing a 2D interpolation of the data points in Fig. 3a and b in the heating part of the cycles we obtained the three surfaces shown in Fig. 3a–c.

We first performed the interpolation of I_d and I_l in T with a linear function because the variation on I_d (T) and I_l (T) is very smooth. At this point we subtracted the I_p curve from the I_l to obtain I_p. The use of a linear interpolation avoids artefacts in the subtraction. We then performed exponential interpolation in time (a linear interpolation on the logarithm of the current) to obtain the three surfaces.

4.5. Error analysis

The error propagation of I_l and I_d into I_p was calculated by the equation:

$$\sigma_{I_p}^2 = \sigma_{I_l}^2 + \sigma_{I_d}^2 - 2 \cdot \mathrm{cov}[I_l, I_d] \quad (6)$$

As the sourcemeter measures consecutive I_d and I_l values, which are in the same range, we consider $\sigma_{I_l} = \sigma_{I_d}$. For uncorrelated noise (i.e. thermal/shot noise) $\mathrm{cov}[I_l, I_d] = 0$, thus the error in I_p calculation is: $\sigma_{I_p} = \sqrt{2} \cdot \sigma_{I_d}$ (Table 1).

Table 1
Summarizes the relevant values for the calculation of the signal to noise ratio (SNR).

Time→	9061 (s)	67287 (s)	Note
Range I_d	2–12 nA	0.6–1.4 nA	Data of Fig. 4
Range I_p	0.1–0.4 nA	0.06–0.35 nA	Data of Fig. 4
$(I_l - I_d)/I_d$	5–3.3%	10–25%	
σ_{I_d}	<6pA rms	<2pA rms	Measured current noise in the same range and same conditions than the I_d
SNR (I_p)	>11	>21	Calculated as $\frac{I_p}{\sqrt{2}\cdot\sigma_{I_d}}$

Acknowledgements

The research leading to these results has received funding from the European Community Seventh Framework Programme (FP7/2007-2013) under grant agreement No: 212311 of the ONE-P project. MC and PS are supported by ESF-EURYI DYMOT. The authors gratefully thank A. Brillante for useful discussions.

References

[1] S. Chandrasekhar, G.S. Ranganath, Rep. Prog. Phys. 53 (1990) 57.
[2] Z. An, J. Yu, S.C. Jones, S. Barlow, S. Yoo, B. Domercq, P. Prins, L.D.A. Siebbeles, B. Kippelen, S.R. Marder, Adv. Mater. 17 (2005) 2580.
[3] A.M. van de Craats, J.M. Warman, M.P. de Haas, D. Adam, J. Simmerer, D. Haarer, P. Schuhmacher, Adv. Mater. 8 (1996) 823.
[4] J.M. Warman, M.P. de Haas, G. Dicker, F.C. Grozema, J. Piris, M.G. Debjie, Chem. Mater. 16 (2004) 4600.
[5] M.G. Debije, J. Piris, M.P. de Haas, J.M. Warman, Ž. Tomović, C.D. Simpson, M.D. Watson, K. Müllen, J. Am. Chem. Soc. 126 (2004) 4641.
[6] W. Pisula, A. Menon, M. Stepputat, I. Lieberwirth, U. Kolb, A. Tracz, H. Sirringhaus, T. Pakula, K. Müllen, Adv. Mater. 17 (2005) 684.
[7] A.M. van de Craats, N. Stutzmann, O. Bunk, M.M. Nielsen, M. Watson, K. Müllen, H.D. Chanzy, H. Sirringhaus, R.H. Friend, Adv. Mater. 15 (2003) 495.
[8] D. Adam, P. Schuhmacher, J. Simmerer, L. Haussling, K. Siemensmeyer, K.H. Etzbach, H. Ringsdorf, D. Haarer, Nature 371 (1994) 141.
[9] H. Iino, J. Hanna, R.J. Bushby, B. Movaghar, B.J. Whitaker, M.J. Cook, Appl. Phys. Lett. 87 (2005) 132102.
[10] C.F. van Nostrum, R.J.M. Nolte, Chem. Commun. 21 (1996) 2385.
[11] F.I. Bohrer, A. Sharoni, C. Colesniuc, J. Park, I.K. Schuller, A.C. Kummel, W.C. Trogler, J. Am. Chem. Soc. 129 (2007) 5640.
[12] M. Cavallini, A. Calò, P. Stoliar, J.C. Kengne, S. Martins, F.C. Matacotta, F. Quist, G. Gbabode, N. Dumont, Y.H. Geerts, F. Biscarini, Adv. Mater. 46 (2009) 4688.
[13] A. Fechtenkötter, N. Tchebotareva, M. Watson, K. Müllen, Tetrahedron 57 (2001) 3769.
[14] R.I. Gearba, A.I. Bondar, B. Goderis, W. Bras, D.A. Ivanov, Chem. Mater. 17 (2005) 2825.
[15] X. Crispin, J. Cornil, R. Friedlein, K.K. Okudaira, V. Lemaur, A. Crispin, G. Kestemont, M. Lehmann, M. Fahlman, R. Lazzaroni, Y. Geerts, G. Wendin, N. Ueno, J.-L. Brédas, W.R. Salaneck, J. Am. Chem. Soc. 126 (2004) 11889.
[16] S. Sergeyev, W. Pisula, Y.H. Geerts, Chem. Soc. Rev. 36 (2007) 1902.
[17] V. Lemaur, D.A. Da Silva Filho, V. Coropceanu, M. Lehmann, Y. Geerts, J. Piris, M.G. Debjie, A.M. van de Craats, K. Senthilkumar, L.D.A. Siebbeles, J.M. Warman, J.-L. Brédas, J. Cornil, J. Am. Chem. Soc. 126 (2004) 3271.
[18] J. Cornil, V. Lemaur, J.P. Calbert, J.L. Brédas, Adv. Mater. 14 (2002) 726.
[19] J.L. Brédas, D. Beljonne, V. Coropceanu, J. Cornil, Chem. Rev. 104 (2004) 4971.
[20] J. Tant, Y.H. Geerts, M. Lehmann, V. de Cupere, G. Zucchi, B.W. Laursen, T. Bjørnholm, V. Lemaur, V. Marcq, A. Burquel, E. Hennebicq, F. Gardebien, P. Viville, P. Beljonne, R. Lazzaroni, J. Cornil, J. Phys. Chem. B 109 (2005) 20315.
[21] X. Feng, V. Marcon, W. Pisula, M.R. Hansen, J. Kirkpatrick, F. Grozema, D. Andrienko, K. Kremer, K. Müllen, Nat. Mater. 8 (2009) 421.
[22] Y. Olivier, L. Muccioli, V. Lemaur, Y.H. Geerts, C. Zannoni, J. Cornil, J. Phys. Chem. B 13 (2009) 14102.
[23] A.M. van de Craats, J.M. Warman, Adv. Mater. 13 (2001) 130.
[24] I.O. Shklyarevskiy, P. Jonkheijm, N. Stutzmann, D. Wasserberg, H.J. Wondergem, P.C.M. Christianen, A.P.H.J. Schenning, D.M. de Leeuw, Ž. Tomović, J. Wu, K. Müllen, J.C. Maan, J. Am. Chem. Soc. 127 (2005) 16233.
[25] C. Deibel, D. Janssen, P. Heremans, V. de Cupere, Y. Geerts, M.L. Benkhedir, G.J. Adriaenssens, Org. Electron. 7 (2006) 495.
[26] L. Schmidt-Mende, A. Fechtenkötter, K. Müllen, E. Moons, R.H. Friend, J.D. MacKenzie, Science 293 (2001) 1119.
[27] A. Calò, P. Stoliar, M. Cavallini, S. Sergeyev, Y.H. Geerts, F. Biscarini, J. Am. Chem. Soc. 130 (2008) 11953.
[28] J.D. Wright, Prog. Surf. Sci. 31 (1989) 1.
[29] J. Yuan, J. Zhang, J. Wang, D. Yan, W. Xu, Thin Solid Films 450 (2004) 316.
[30] Q. Zhou, R.H. Gould, Thin Solid Films 317 (1998) 432.
[31] M. Funahashi, J. Hanna, Chem. Phys. Lett. 397 (2004) 319.
[32] R. James, G. Stojmenovik, C. Desimpel, F.A. Fernández, S.E. Day, K. Neyts, J. Display Technol. 2 (2006) 237.
[33] V. De Cupere, J. Tant, P. Viville, R. Lazzaroni, W. Osikowicz, W.R. Salaneck, Y.H. Geerts, Langmuir 22 (2006) 7798.
[34] A. Calò, P. Stoliar, M. Cavallini, Y.H. Geerts, F. Biscarini, Rev. Sci. Instrum. 81 (2010) 033907.
[35] G.L. Pakhomov, D.M. Gaponova, A.Yu. Luk'yanov, E.S. Leonov, Proceedings of the Conference "Nanophotonics 2004" Nizhni Novgorod, Russia 2 (2004) 6.
[36] G. Schweicher, G. Gbabode, F. Quist, O. Debever, N. Dumont, S. Sergeyev, Y.H. Geerts, Chem. Mater. 21 (2009) 5867.
[37] N.W. Ashcroft, N.D. Mermin, Solid State Physics, Harcourt, Orlando, 1976.
[38] T.S. Shafai, R.D. Gould, Thin Solid Films 515 (2006) 1138.
[39] D.F. Barbe, C.R. Westgate, J. Chem. Phys. 52 (1970) 4046.
[40] S.M. Sze, K.K. Ng, Physics of Semiconductor Devices, John Wiley & Sons, 1981.
[41] D. Markovitsi, S. Marguet, J. Bondkowski, S. Kumar, J. Phys. Chem. B 105 (2001) 1299.
[42] S.B. Lei, J. Wang, Y.H. Dong, C. Wang, L.J. Wan, C.L. Bai, Surf. Interface Anal. 34 (2002) 767.
[43] V. Corradini, C. Menozzi, M. Cavallini, F. Biscarini, M.G. Betti, C. Mariani, Surf. Sci. 532 (2003) 249.
[44] C. Menozzi, V. Corradini, M. Cavallini, F. Biscarini, M.G. Betti, C. Mariani, Thin Solid Films 428 (2003) 227.
[45] D.A. Serban, P. Greco, S. Melinte, S. Vlad, C.A. Dutu, S. Zacchini, M.C. Iapalucci, F. Biscarini, M. Cavallini, Small 5 (2009) 1117.
[46] P. Leclere, M. Surin, R. Lazzaroni, A.F.M. Kilbinger, O. Henze, P. Jonkheijm, F. Biscarini, M. Cavallini, W.J. Feast, E.W. Meijer, A. Schenning, J. Mater. Chem. 14 (2004) 1959.
[47] F. Yakuphanoglu, M. Durmuş, M. Okutan, O. Köysal, V. Ashen, Physica B 373 (2006) 262.